Molecular Biology of the Cell
Vol. 14, 3400–3413, August 2003

The Role of Subunit Assembly in Peripherin-2 Targeting to Rod Photoreceptor Disk Membranes and Retinitis Pigmentosa

Christopher J.R. Loewen,* Orson L. Moritz,† Beatrice M. Tam,† David S. Papermaster,† and Robert S. Molday*‡§

*Department of Biochemistry and Molecular Biology and the ‡Department of Ophthalmology, University of British Columbia, Vancouver, British Columbia, Canada V6T 1Z3; and †Department of Neuroscience, University of Connecticut Health Center, Farmington, Connecticut 06032-3705

Submitted February 10, 2003; Revised March 19, 2003; Accepted April 9, 2003
Monitoring Editor: Benjamin Glick

Peripherin-2 is a member of the tetraspanin family of membrane proteins that plays a critical role in photoreceptor outer segment disk morphogenesis. Mutations in peripherin-2 are responsible for various retinal degenerative diseases including autosomal dominant retinitis pigmentosa (ADRP). To identify determinants required for peripherin-2 targeting to disk membranes and elucidate mechanisms underlying ADRP, we have generated transgenic *Xenopus* tadpoles expressing wild-type and ADRP-linked peripherin-2 mutants as green fluorescent fusion proteins in rod photoreceptors. Wild-type peripherin-2 and P216L and C150S mutants, which assemble as tetramers, targeted to disk membranes as visualized by confocal and electron microscopy. In contrast the C214S and L185P mutants, which form homodimers, but not tetramers, were retained in the rod inner segment. Only the P216L disease mutant induced photoreceptor degeneration. These results indicate that tetramerization is required for peripherin-2 targeting and incorporation into disk membranes. Tetramerization-defective mutants cause ADRP through a deficiency in wild-type peripherin-2, whereas tetramerization-competent P216L peripherin-2 causes ADRP through a dominant negative effect, possibly arising from the introduction of a new oligosaccharide chain that destabilizes disks. Our results further indicate that a checkpoint between the photoreceptor inner and outer segments allows only correctly assembled peripherin-2 tetramers to be incorporated into nascent disk membranes.

INTRODUCTION

The outer segment is a specialized compartment of retinal photoreceptor cells that mediates phototransduction. In rod cells, it consists of an ordered stack of disks enclosed by a separate plasma membrane. Each disk is made up of two flattened membranes circumscribed by a hairpin rim region with one or more incisures. Rod outer segments (ROS) undergo a continuous renewal process. Membrane proteins synthesized in the rod inner segment are translocated through a connecting cilium and incorporated into newly formed disks at the proximal end of the ROS, whereas packets of aged disks are shed at the distal end and removed by retinal pigment epithelial cell–mediated phagocytosis (Bok, 1985).

Peripherin-2 (also known as peripherin/rds) is a membrane protein localized to the rims and incisures of photoreceptor disks (Molday *et al.*, 1987; Arikawa *et al.*, 1992). It plays a crucial role in outer segment morphogenesis because *rds* mice homozygous for the disrupted peripherin-2 gene fail to develop outer segments and heterozygous mice produce highly disorganized disk structures (Sanyal and Jansen, 1981; Hawkins *et al.*, 1984; Travis *et al.*, 1989, 1992; Connell *et al.*, 1991). The importance of peripherin-2 in photoreceptor viability is further highlighted by the finding that >40 different mutations in peripherin-2 have been linked to human retinopathies, including autosomal dominant retinitis pigmentosa (ADRP), a retinal degenerative disease characterized by night blindness, progressive loss of vision, and photoreceptor cell death (Farrar *et al.*, 1991; Kajiwara *et al.*, 1991; Saga *et al.*, 1993; Weleber *et al.*, 1993).

Article published online ahead of print. Mol. Biol. Cell 10.1091/mbc.E03–02–0077. Article and publication date are available at www.molbiolcell.org/cgi/doi/10.1091/mbc.E03–02–0077.

§ Corresponding author. E-mail address: molday@interchange.ubc.ca.

Abbreviations used: GFP, green fluorescent protein; ROS, rod outer segments; ADRP, autosomal dominant retinitis pigmentosa; WT, wild-type; DTT, dithiothreitol.

Peripherin-2 is a member of the tetraspanin family of membrane proteins characterized by four transmembrane segments and a large intradiskal (EC-2) domain between the third and fourth membrane-spanning segments (see Figure 1; Connell and Molday, 1990; Travis *et al.*, 1991; Hemler, 2001; Seigneuret *et al.*, 2001). The EC-2 domain contains one N-linked glycosylation site and seven conserved cysteine residues that participate in intramolecular and intermolecular disulfide bonds important for protein folding and subunit assembly (Goldberg *et al.*, 1998; Loewen and Molday, 2000).

In mammalian photoreceptors, peripherin-2 associates with itself and with rom-1, a related tetraspanin protein, to form a mixture of core homo- and heterotetramers (Goldberg and Molday, 1996b; Loewen and Molday, 2000; Loewen *et al.*, 2001). These tetramers further link together through intermolecular disulfide bonds to form octamers and higher order oligomers believed to be crucial for disk rim formation (Loewen and Molday, 2000; Wrigley *et al.*, 2000). In contrast to peripherin-2, rom-1 plays a relatively minor role in disk morphogenesis and structure because rom-1 knockout mice develop outer segments that are only modestly altered in appearance (Clarke *et al.*, 2000). Furthermore, rom-1 is absent in lower vertebrates including amphibians (Kedzierski *et al.*, 1996).

Several recent studies have examined the effect of disease-causing missense mutations on the biochemical properties of peripherin-2 and the structure of ROS. The C214S peripherin-2 mutation linked to a monogenic form of ADRP is misfolded and defective in its ability to form core tetramers (Goldberg and Molday, 1996a; Goldberg *et al.*, 1998; Loewen *et al.*, 2001). The L185P peripherin-2 mutation associated with a digenic form of ADRP assembles with wild-type (WT) peripherin-2 and rom-1 to form functional heterotetramers, but is unable to self-associate into tetramers. Transgenic mice harboring disease-linked mutations generally show disorganized outer segments that correlate with photoreceptor degeneration (Kedzierski *et al.*, 1997, 2001). However, because the mutant protein could not be distinguished from endogenous WT peripherin-2 in these mice, the effect of disease-linked mutations on peripherin-2 targeting to outer segment disks could not be determined. Hence, it is unclear if defective targeting of mutant peripherin-2 to outer segment disk membranes contributes to the cellular mechanism underlying ADRP.

In the present study we have generated transgenic *X. laevis* tadpoles expressing WT, C214S, P216L, L185P, and C150S peripherin-2 green fluorescent fusion protein (GFP) to identify determinants responsible for the targeting of peripherin-2 to ROS disks and to define cellular and molecular mechanisms responsible for ADRP. Here, we show that peripherin-2 core tetramer formation is required for proper targeting and incorporation of peripherin-2 into newly formed disks membranes. We also provide evidence that ADRP caused by tetramerization-defective peripherin-2 mutations (C214S and L185P) occurs through a mechanism involving a deficiency in WT peripherin-2, whereas ADRP associated with the tetramer-competent P216L peripherin-2 mutation takes place through a dominant negative mechanism.

MATERIALS AND METHODS

Generation of WT and Mutant Peripherin-2-GFP Constructs

Xenopus laevis peripherin-2 (Xrds-38) cDNA was cloned from total retinal RNA by PCR using sequence-specific primers based on the Xrds-38 sequence (Kedzierski *et al.*, 1996). The sequence differed slightly from the published Xrds-38 sequence (Kedzierski *et al.*, 1996). Five amino acid differences (A78, A92, D187, F188, and S189) were found that are conserved in mouse, rat, cat, dog, bovine, and human orthologues, suggesting that these amino acids are bona fide residues of *Xenopus* peripherin-2 (Figure 1A). The GenBank accession number is AY062004.

The *X. laevis* peripherin-2-GFP construct for COS-1 cell expression was created by PCR, removing the stop codon and cloning in frame into the *Xho*I and *Eco*RI sites of peGFP-N2 (CLONTECH Laboratories, Inc., Palo Alto, CA). For transgenic *X. laevis* expression, the *Xho*I-*Not*I fragment of *Xenopus* peripherin-2-GFP (including GFP) was subcloned into the *Xho*I and *Not*I sites of XOP1.3-eGFP-N1. This plasmid was derived from peGFP-N1 by replacing the CMV promoter with a portion of the *X. laevis* opsin promoter (Batni *et al.*, 2000; Tam *et al.*, 2000). Quickchange PCR-based mutagenesis (Stratagene, La Jolla, CA) was used to introduce the L185P, C214S, P216L, and C150S mutations. Bovine WT-peripherin-2-GFP and C214S-peripherin-2-GFP fusion constructs were created in a similar manner. All PCR products and constructs were verified by sequencing. Transgenic expression constructs were linearized by *Sfo*I digestion.

mAb Production

Oligonucleotides coding for the *Xenopus* peripherin-2 C-terminal amino acid sequence KDTIKSSWELVKSMGKLNKVE were synthesized with appropriate restriction sites and cloned into the pGEX vector. The GST fusion protein, expressed in *Escherichia coli*, was purified on a glutathione-Sepharose affinity column and used to immunize Swiss Webster mice for generation of the Xper5A11 mAb as previously described (MacKenzie and Molday, 1982).

Production of Transgenic X. laevis

Transgenic frogs were generated using a modified protocol (Moritz *et al.*, 1999) based on the method of Kroll and Amaya (1996). *X. laevis* sperm nuclei were incubated with 0.3× high-speed egg extract, 0.05 U restriction enzyme, and 100–200 ng linearized plasmid DNA. The reaction mixture was then diluted to 0.3 nuclei/nl and 10 nl was injected per egg. The resulting embryos were kept at 18°C in 0.1× Marc's modified Ringer, 6% Ficoll solution for 48 h and then switched to 0.1× Gerhart's Ringer solution. At 5–6 d postfertilization (dpf) roughly corresponding to stages 40–42, tadpoles were screened for GFP expression using a Leica MZ8 dissecting microscope (Leica Microsystems, Wetzlar, Germany) equipped with epifluorescence optics and a GFP filter set. Animals were immobilized in glass Pasteur pipettes and tadpoles expressing GFP were identified by the green fluorescence emitted from their eyes. At 14 dpf, the transgenic tadpoles were placed in tanks with 0.1× Gerhart's Ringer solution and reared at 18°C on a 12/12 h light/dark cycle. Adult *X. laevis* were obtained from Nasco or *Xenopus* Express (Plant City, FL).

Immunocytochemistry

For *X. laevis* immunofluorescence studies, tadpoles were sacrificed between 14 and 28 dpf (stage 48–62). After immobilizing the tadpoles in 0.02% Tricaine, their eyes were excised and fixed in 4% paraformaldehyde, sodium phosphate buffer, pH 7.5, overnight. Fixed eyes were embedded in OCT tissue embedding medium (Tissue-Tek) and frozen in a dry ice/isopentane bath. Cryostat sections (14 μm) were blocked (10% BSA, 0.1% Triton X-100 in PBS) and labeled overnight with 0.1 mg/ml Texas Red–conjugated wheat germ agglutinin (TR-WGA; Molecular Probes, Eugene, OR) and 0.01

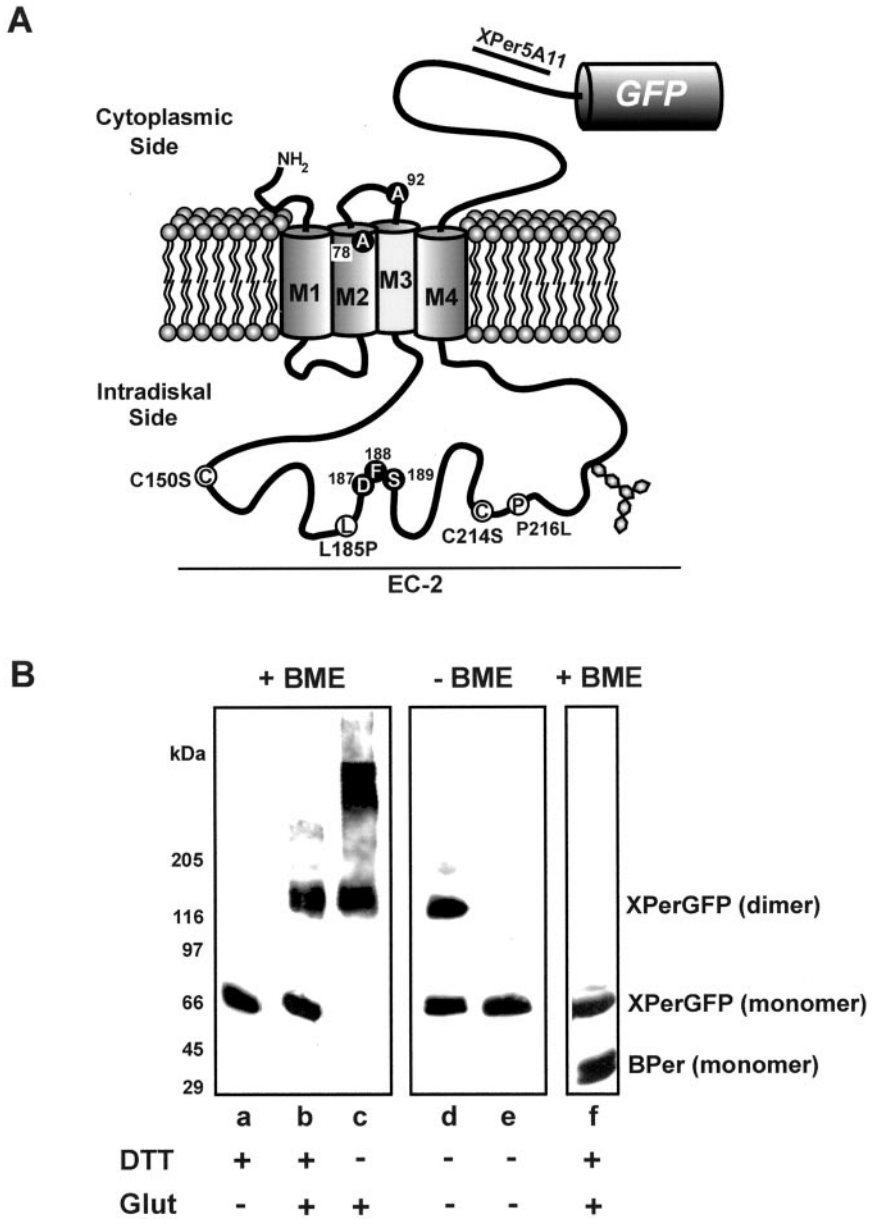

Figure 1. Analysis of *Xenopus* peripherin-2-GFP fusion protein. (A) Topological model for *Xenopus* peripherin-2 showing the location of the GFP fusion protein, the epitope for the Xper5A11 mAb, mutations analyzed in this study (white circles), and amino acids that differ from the published sequence (black circles). (B) Western blots of *Xenopus* peripherin-2-GFP expressed in COS-1 cells. COS-1 membranes were preincubated with or without DTT, solubilized in Triton X-100, treated with or without glutaraldehyde (Glut), and fractionated on SDS gels under reducing (+BME, β-mercaptoethanol) or nonreducing (-BME) conditions. Lanes a–d: WT *Xenopus* peripherin-2-GFP labeled with an anti-GFP antibody. Lane e: C150S *Xenopus* peripherin-2-GFP labeled with anti-GFP antibody. Lane f: Coexpression and coimmunoprecipitation of *Xenopus* peripherin-2-GFP (XPerGFP) and bovine peripherin-2 (BPer) with bovine specific Per2B6-Sepharose. Western blots were labeled with an anti-GFP antibody to detect XperGFP and the Per2B6 antibody to detect BPer.

mg/ml Hoescht 33342 stain (Sigma-Aldrich, Oakville, ON) to label photoreceptor membranes and nuclei, respectively. Sections were also labeled with anti-*Xenopus* peripherin-2 mAb Xper5A11. Labeling was done in the presence of 1 mM $CaCl_2$, 1 mM $MgCl_2$, 1% BSA, and 0.1% Triton X-100 in PBS for visualization under a Zeiss 510 confocal laser scanning microscope (Thornwood, NY). At least three transgenic animals were examined for each construct.

For immunoelectron microscopy, transgenic tadpoles were killed at 14 and 28 dpf (stage 48–62) and fixed overnight in 4% paraformaldehyde, 0.1 M sodium phosphate buffer, pH 7. The eyes were embedded in LR White resin, incubated overnight with a rabbit anti-GFP polyclonal antibody (Clontech Laboratories, Inc.) diluted 1:100 in 1% bovine serum albumin (BSA), 0.1 M Tris, pH 7.4, and labeled for 1 h with anti-rabbit Ig-gold (10 nm; British BioCell International, Cardiff, United Kingdom) diluted 1:5 in 0.1 M Tris, pH 7.4, 1% BSA. A minimum of two transgenic animals was examined for each construct.

COS-1 Cell Expression and Analysis

COS-1 cells (ca. 6×10^5 cells/100-mm dish) were transfected with a total of 30 μg of pcDNAI/amp containing the appropriate peripherin-2 construct as previously described (Goldberg *et al.*, 1995). For immunofluorescence studies, the cells transfected with GFP constructs were fixed and labeled with an anticalnexin antibody (Stressgene, Victoria, BC) as an ER marker for analysis by confocal scanning microscopy. For biochemical studies, transfected COS-1 cells were washed and incubated in PBS in the presence (reduced) or absence (nonreduced) of 20 mM dithiothreitol (DTT) for 90 min at 25°C. The cells were solubilized with an equal volume of PBS (pH

7.4) containing 2% Triton X-100, 80 mM *N*-ethyl maleimide, and phenyl methyl sulfonyl fluoride for 10 min on ice, and the detergent extract was centrifuged at 90,000 × *g* for 30 min at 4°C to remove any aggregated material and analyzed by SDS gels and Western blotting. Bovine peripherin-2 was purified on a Per2B6-Sepharose matrix as previously described (Loewen and Molday, 2000).

For velocity sedimentation experiments the solubilized extract was applied to 5–20% (wt/wt) sucrose gradients in PBS containing 0.1% Triton X-100 (Loewen and Molday, 2000). After centrifugation for 16 h at 50,000 rpm in a Beckman TLS-55 rotor (Beckman, Mississauga, ON) at 4°C, the bottom of the centrifuge tube was punctured and fractions were analyzed on Western blots.

Protein cross-linking was performed on untreated or DTT-treated detergent-solubilized cell extracts with 0.005% glutaraldehyde for 15 min at 37°C. Samples in the absence or presence of 5% β-mercaptoethanol were fractionated on 6% or 8% SDS-polyacrylamide gels. Western blots were labeled with Per 2B6 mAb specific for bovine peripherin-2 (Molday *et al.*, 1987) and a GFP polyclonal antibody (Clontech Laboratories, Inc.) specific for the GFP fusion protein for detection by ECL. PNGase F deglycosylation of peripherin-2 was carried out as recommended by the manufacturer (New England BioLabs, Mississauga, ON).

RESULTS

Biochemical Properties of Peripherin-2-GFP

Peripherin-2 from ROS membranes and COS-1 cells exists as core noncovalent tetramers (Goldberg and Molday, 1996b; Loewen and Molday, 2000). A significant fraction of these tetramers link together through C150 mediated disulfide bonds to form higher-order oligomers (Loewen and Molday, 2000). As a result, peripherin-2 migrates as a 35-kDa monomer on SDS gel under disulfide reducing conditions and a mixture of monomers and disulfide-linked dimers under nonreducing conditions.

We have expressed *Xenopus* and bovine peripherin-2-GFP fusion proteins in COS-1 cells in order to determine the effect of the C-terminal GFP on its oligomeric properties. Like the endogenous protein, *Xenopus* and bovine peripherin-2-GFP fusion proteins migrated on SDS gels as monomers under reducing conditions (Figure 1B, lane a) and a mixture of monomers and dimers under nonreducing conditions (Figure 1B, lane d). Replacement of cysteine at position 150 with serine (C150S) in *Xenopus* as well as bovine peripherin-2-GFP abolished dimer formation (Figure 1B, lane e) consistent with the role of C150 residues in intermolecular disulfide bonding. Glutaldehyde cross-linking of *Xenopus* peripherin-2-GFP resulted in a mixture of monomers and dimers under reducing conditions (Figure 1B, lane b) and dimers and higher molecular weight species under nonreducing conditions (Figure 1B, lane c) as previously reported for bovine peripherin-2 (Loewen and Molday, 2000). When coexpressed in COS-1 cells, *Xenopus* peripherin-2-GFP coprecipitated with bovine peripherin-2 on a Per2B6 immunoaffinity matrix specific for bovine peripherin-2, indicating that *Xenopus* and bovine peripherin-2 assembled into multisubunit complexes (Figure 1B, lane f). Together, these results indicate that GFP fused to the C termini of peripherin-2 does not affect the subunit assembly of peripherin-2.

Immunolocalization of Endogenous Peripherin-2 in **Xenopus laevis**

Confocal scanning microscopy was used to visualize the distribution of peripherin-2 in a *Xenopus* retina labeled with a peripherin-2 mAb. Figure 2, A and B, shows that labeling was confined to rod and cone outer segments. The vertical striations observed in ROS and the restricted labeling to one edge of cone outer segments are indicative of peripherin-2 localization to the rims and incisures of disk membranes (Molday *et al.*, 1987; Arikawa *et al.*, 1992; Kedzierski *et al.*, 1996).

Expression of Xenopus and Bovine WT Peripherin-2-GFP in Xenopus Rods

tk;2Xenopus peripherin-2-GFP under the control of the *Xenopus* rhodopsin promoter was found only in the outer segments of rod photoreceptors (Figure 2, C and D). The contiguous row of photoreceptor nuclei and long uniform appearance of the ROS indicated that peripherin-2-GFP expression did not affect outer segment structure or induce retinal degeneration. Furthermore, the peripherin-2-GFP was observed in phagosomes within the retinal pigment epithelial cells, indicating that normal disk shedding and phagocytosis had occurred.

Peripherin-2-GFP expression varied along the length of a ROS, between rod photoreceptors within the retina and from animal to animal (Figure 2, C and E). A similar variation in protein expression has been observed previously in transgenic *X. laevis* tadpoles expressing rhodopsin-GFP (Tam *et al.*, 2000; Moritz *et al.*, 2001b). This variable rod expression has been attributed to random transgene silencing, with a probability dependent on the chromosomal location of transgene integration (position-effect variegation). Together with the unique mechanisms of ROS renewal, transient silencing results in bands of varying fusion protein concentration (Karpen, 1994; Moritz *et al.*, 2001b). This variation permitted us to examine the effects of different expression levels within the same retina, and even within the same ROS.

In regions of moderate expression, peripherin-2-GFP fluorescence showed vertical striations in longitudinal sections and a scalloped appearance in transverse sections (Figure 2E), similar to endogeneous peripherin-2 and characteristic of protein targeting to the disk rims and incisures. In regions of high expression, GFP fluorescence saturated the ROS and the distinctive striated pattern of fluorescence was lost.

The distribution of peripherin-2-GFP was mapped more precisely by electron microscopy using an anti-GFP antibody with postembedding immunogold labeling. In longitudinal and transverse sections, peripherin-2-GFP was confined to the disk rims and incisures of ROS at moderate expression levels (Figure 2, F and G). In regions of high expression, peripherin-2-GFP was also observed in the disk lamellae (Figure 2H). Intense immunogold labeling correlated with a reduction in the diameter of the ROS and the presence of smaller, more disorganized disks.

Bovine peripherin-2-GFP was also expressed in *X. laevis* in order to determine if the requirements for targeting of peripherin-2 to ROS are conserved between mammalian and amphibian species. Like *Xenopus* peripherin-2-GFP, the bovine fusion protein targeted to the outer segments and showed partial colocalization with endogenous *Xenopus* peripherin-2 as shown in Figure 3D.

Transgenic Expression of C214S Peripherin-2-GFP

The disease-linked C214S peripherin-2 mutation prevents tetramer formation, but does not affect dimerization of pe-

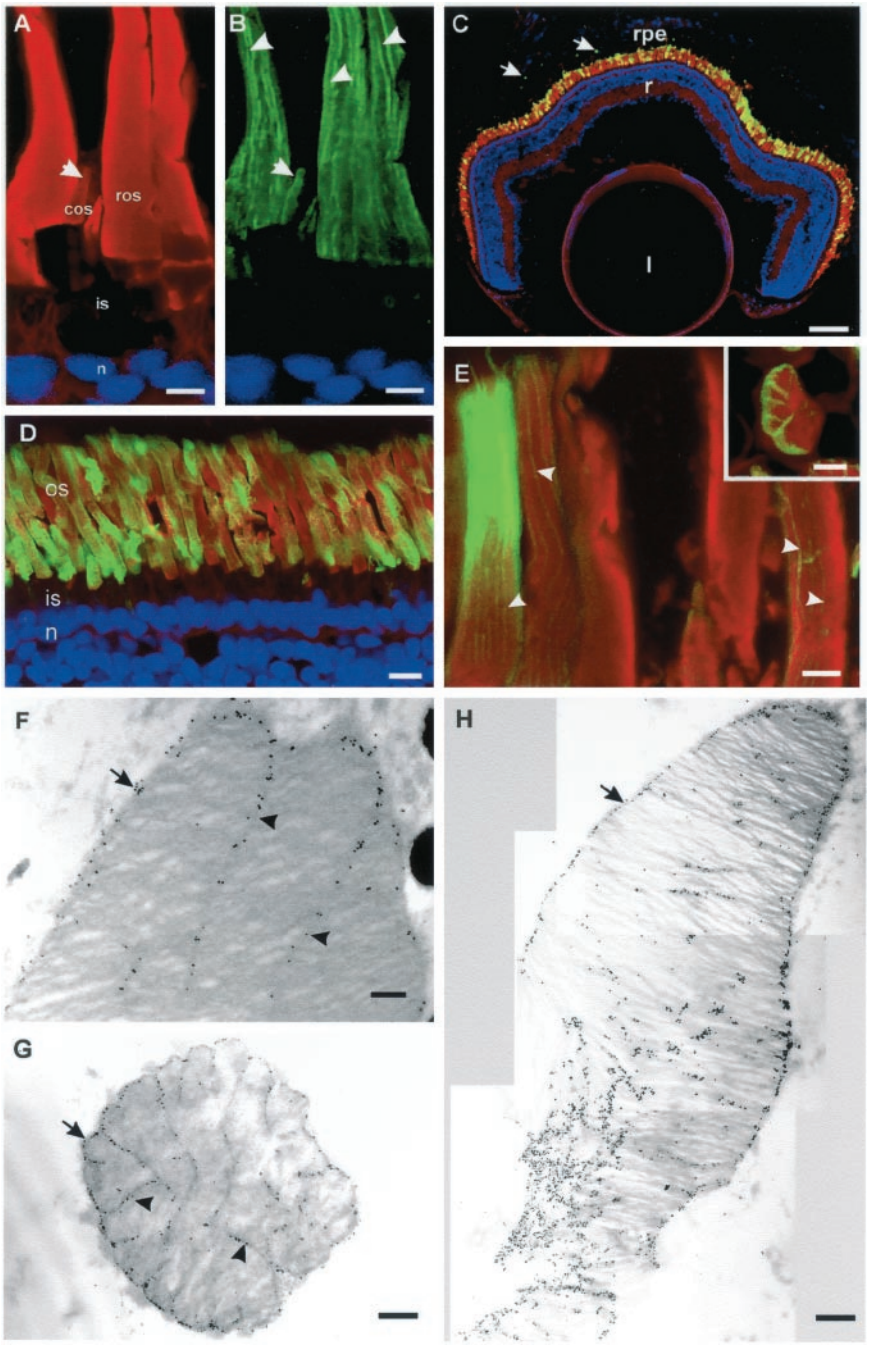

Figure 2. Endogenous peripherin-2 and WT peripherin-2-GFP localize to the ROS disk rims and incisures. (A and B) *X. laevis* retina was labeled with TR-WGA (red) and antiperipherin-2 Xper5A11 antibody (green) and stained with Hoescht 33342 (blue). (A) TR-WGA labeling of glycoproteins in rod (ros) and cone (cos) outer segments; inner segment (is) and nuclei (n) are not labeled; (B) peripherin-2 labeling along the disk rims and incisures (arrowheads) and one edge of the cos (arrow). Bar, 5 μm. (C–E) Cryosections of 4-week-old tadpole eyes expressing WT *Xenopus* peripherin-2-GFP (green) and stained with TR-WGA (red) and Hoescht 33342 (blue). (C) Retina expressing *Xenopus* peripherin-2-GFP in ROS. Fusion protein is also present in phagosomes in retinal pigment epithelial cells (arrow). l, lens; r, retina; rpe, retinal pigment epithelium; Bars, 100 μm. (D and E) Micrographs of retinas expressing *Xenopus* peripherin-2-GFP at higher magnification showing peripherin-2-GFP localized to the ROS disk rims and incisures (arrowheads). Bars, 10 μm (D) and 5 μm (E); (Inset) Cross section of a ROS. Bar, 1 μm. All detectable WT peripherin-2-GFP localized to the ROS. F-H. Electron micrographs of retina labeled for *Xenopus* peripherin-2-GFP with an anti-GFP antibody and immunogold markers. (F) Longitudinal section (Bar, 0.2 μm) and (G) transverse section (Bar, 0.5 μm) of a rod expressing moderate levels of fusion protein. Peripherin-2-GFP is present on the disk rims (arrows) and incisures (arrowheads). (H) Composite longitudinal section of a ROS expressing high levels of the fusion protein. Some missorting of the fusion protein to the disk lamellae and constriction of the rod outer segment is evident. Bar, 0.5 μm.

ripherin-2 (Goldberg *et al.*, 1998). To determine the effect of this mutation on the subcellular localization of peripherin-2, *Xenopus* C214S peripherin-2-GFP was expressed in *Xenopus* rod photoreceptors. Figure 3, A and B, shows that this mutant is retained in the inner segment and cell body of all rods. However, in some cells expressing high levels of the transgene, fusion protein was also detected at the base of their ROS. Photoreceptor degeneration was not evident in animals up to 4 weeks old.

Immunoelectron microscopy confirmed the retention of *Xenopus* C214S peripherin-2-GFP within the inner segment (Figure 3C). Furthermore, a significant amount of the mutant protein was observed to accumulate near the base of the connecting cilium indicating that a portion of the mutant protein passed through the quality control of the ER. The ultrastructure of the ROS appeared normal.

The distribution of bovine C214S peripherin-2-GFP expressed in *X. laevis* retina was also examined. Like *Xenopus*

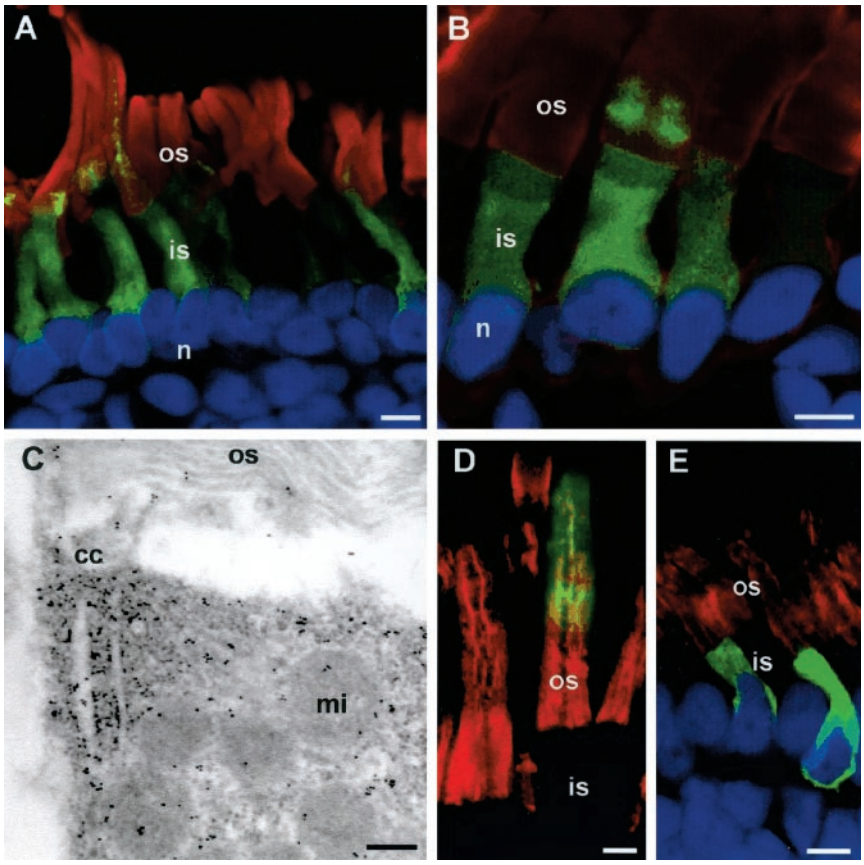

Figure 3. C214S peripherin-2-GFP is retained in the rod inner segment and cell body. (A and B) Confocal micrographs of *Xenopus* retinas expressing *Xenopus* C214S-peripherin-2-GFP (green) and labeled with TR-WGA (red) and Hoescht 33342 (blue). All rod photoreceptors expressing C214S peripherin-2-GFP showed localization of the fusion protein in the rod inner segments and cell bodies; in a small number of high expressing cells, however, some fusion protein is also detected at the base of the ROS. (C) Electron micrograph of immunogold labeling of C214S-peripherin-2-GFP showing protein accumulation near the cilium. (D) Confocal micrograph of a *Xenopus* retina expressing bovine WT-peripherin-2-GFP (green) and labeled for endogenous *Xenopus* peripherin-2 with Xper5A11 antibody (red). The WT bovine fusion protein, like endogeneous *Xenopus* peripherin-2 localizes to the ROS. (E) *Xenopus* retina expressing bovine C214S-peripherin-2-GFP (green) and labeled for endogenous *Xenopus* peripherin-2 (red). The C214S fusion protein does not localize to ROS or affect the targeting of endogenous peripherin-2 to the ROS. os, outer segment; is, inner segment; n, nucleus; cc, connecting cilium; mi, mitochondrion. Bars: (A, B, D, and E) 5 μm; (C) 0.2 μm.

C214S peripherin-2-GFP, the bovine mutant was localized throughout the rod inner segments and cell body, but absent in the ROS (Figure 3E). The targeting of endogenous *Xenopus* peripherin-2 to ROS was unaffected by the presence of bovine C214S peripherin-2-GFP.

Transgenic Expression of P216L Peripherin-2-GFP

The effect of the P216L peripherin-2 mutation, associated with another monogenic form of ADRP, was also examined (Kajiwara *et al.*, 1991). Figure 4A shows the expression pattern of *Xenopus* P216L-peripherin-2-GFP in a tadpole retina. Peripheral rods were long and uniform in appearance, with the fusion protein specifically localized to the outer segments (Figure 4C). By electron microscopy, the ultrastructure of peripheral ROS appeared normal with the P216L peripherin-2-GFP protein specifically targeted to the disk rims and incisures (Figure 4F). In contrast, the central rods were shorter and highly disorganized with an apparent decrease in cell number indicative of photoreceptor degeneration (Figure 4, D and E). Immunoelectron microscopy further showed the presence of the P216L fusion protein in whorls of outer segment disk membranes (Figure 4, G and H).

Transgenic Expression of L185P Peripherin-2-GFP

A L185P mutation in peripherin-2 together with either a null allele or a G113E mutation in rom-1 is responsible for a digenic form of ADRP (Kajiwara *et al.*, 1994). Biochemical studies have shown that this mutant is unable to self-associate into homotetramers, but a significant fraction can interact with WT peripherin-2 and WT rom-1 of mammalian photoreceptors (Goldberg and Molday, 1996a; Loewen *et al.*, 2001). To evaluate the effect of the L185P mutation on the subcellular localization of peripherin-2, we expressed *Xenopus* L185P-peripherin-2-GFP in rods. The mutant GFP fusion protein targeted to both the inner and outer segments of rod cells (Figure 5, A and B). Photoreceptor degeneration was not observed.

Expression of C150S peripherin-2-GFP

The C150S peripherin-2 mutant assembles into noncovalent tetramers, but these core complexes are incapable of forming higher order disulfide-linked oligomers (Loewen and Molday, 2000). To assess the role of disulfide-mediated oligomerization of peripherin-2 in protein targeting and retinal degeneration, we expressed *Xenopus* C150S peripherin-2-GFP in rod cells. Figure 5, C and D, show that the C150S mutant targeted specifically to ROS. Vertical striations characteristic of fusion protein localization to disk incisures, however, were not readily visible with the C150S mutant. Instead, a more mottled labeling pattern was observed, often with the presence of a thick central column of fluorescence. By electron microscopy, C150S peripherin-2 localized to the disk lamellae as well as the rims indicating that some missorting of the protein within the disks had occurred. There

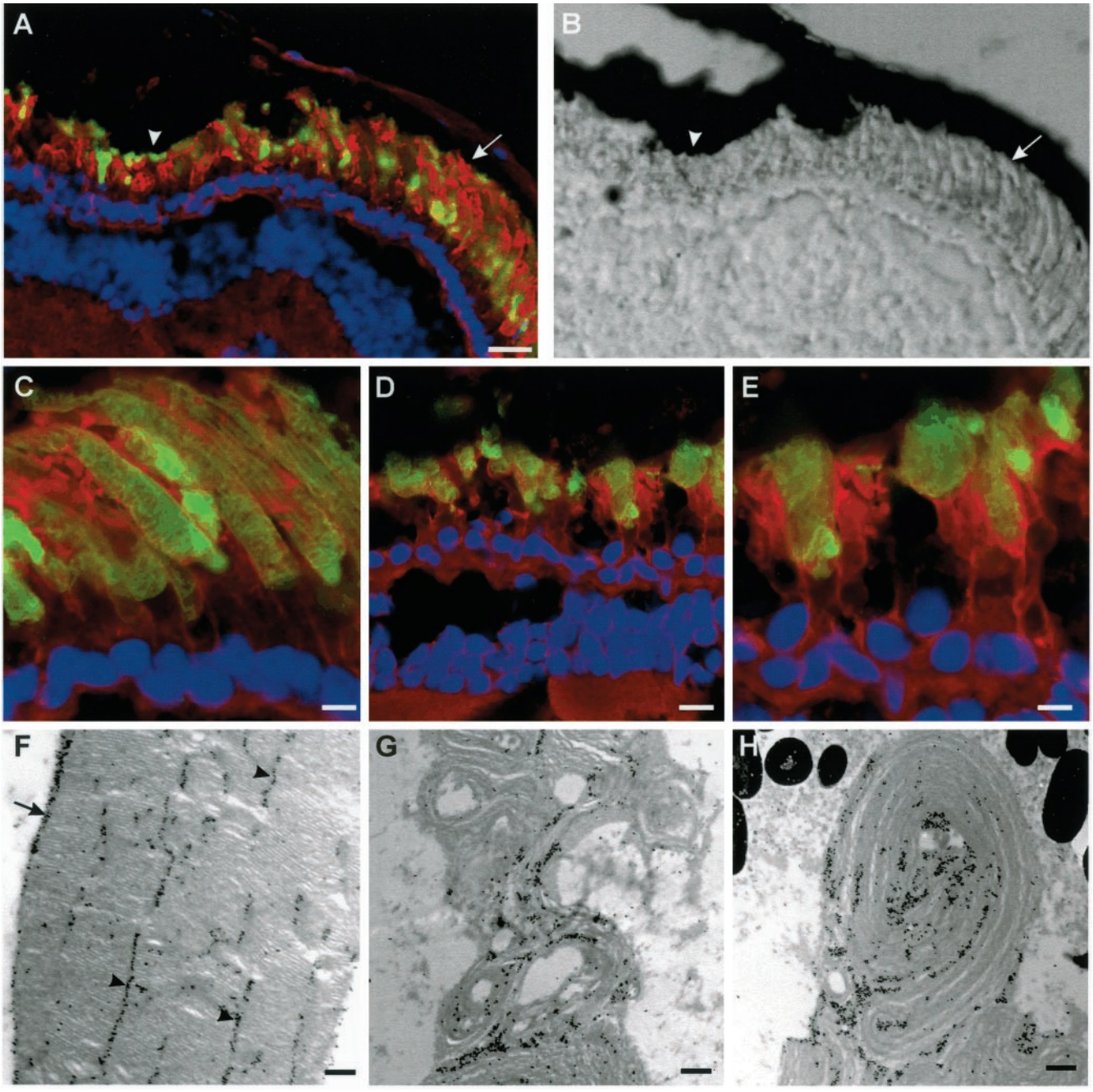

Figure 4. P216L peripherin-2 targets to the ROS and induces degeneration. (A) Fluorescence and (B) corresponding DIC image of a retina expressing *Xenopus* P216L-peripherin-2-GFP (green) and labeled with TR-WGA (red) and Hoescht 33342 (blue). Rods in the peripheral retina (arrow) appear normal while rods in the central retina (arrowhead) have short, highly disorganized outer segments. All detectable P216L fusion protein targets to ROS. Confocal micrographs of peripheral (C) and central (D and E) regions of the same retina show specific targeting of the fusion protein to ROS and degeneration of the central rods. (F–H) Electron micrographs of ROS labeled with an anti-GFP antibody and immunogold particles. (F) ROS from peripheral retina show normal ultrastructure with the P216L mutant protein localized to the disk rims (arrows) and incisures (arrowheads). (G and H) ROS from the central retina appear highly disorganized with whorls of disk membranes with an irregular distribution of fusion protein. ros, rod outer segment; ris, rod inner segment; n, nucleus. Bars: (A and B) 20 μm; (C) 5 μm; (D) 10 μm; (E) 5 μm; (F–H) 0.25 μm.

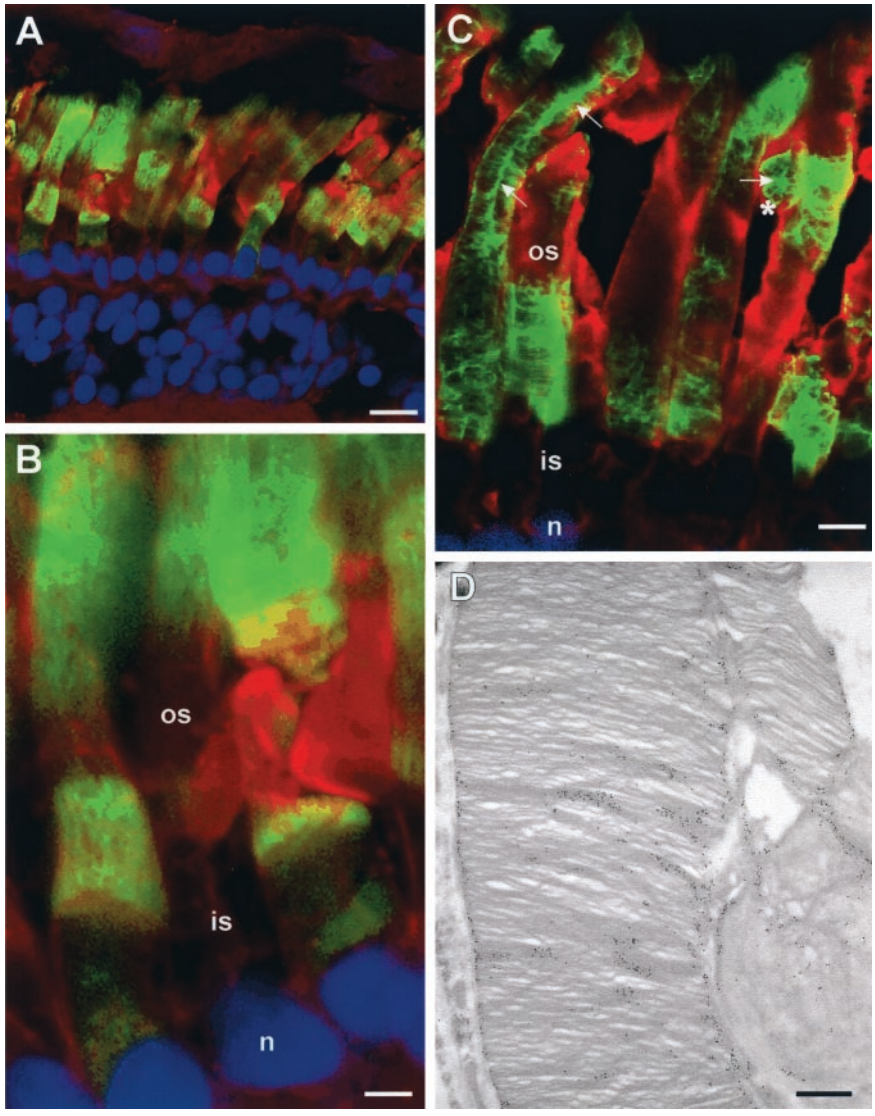

Figure 5. Distribution of L185P and C150S peripherin-2-GFP in rod photoreceptors. (A and B) Retina expressing *Xenopus* L185P peripherin-2-GFP (green) and labeled with TR-WGA (red) and Hoescht 33342 (blue). The L185P mutant is present in ROS in all cells; however, in >25% of the cells the L185P mutant is also present in the inner segment and cell body. (C) Retina expressing *Xenopus* C150S peripherin-2-GFP in ROS. The fusion protein is exclusively localized to the ROS. The vertical striations characteristic of disk incisure localization are not evident; instead a more mottled labeling of the outer segments is observed with some outer segments showing a single vertical column of labeling (arrows; asterisk marks a ROS in cross section). (D) Electron micrograph showing immunogold labeling of the C150S peripherin-2-GFP. Some missorting to the lamellar region of the disks is apparent. ros, rod outer segment; ris, rod inner segment; n, nucleus. Bars: (A and B) 5 μm; (C) 10 μm; (D) 2.5 μm.

was no apparent photoreceptor degeneration in these transgenic tadpoles.

Localization and Biochemical Characterization of P216L and C214S Peripherin-2 Expressed in COS Cells

The subcellular localization of WT and mutant X. *laevis* peripherin-2-GFP expressed in COS-1 cells was examined by confocal microscopy (Figure 6A). WT peripherin-2-GFP exhibited a punctuate appearance indicative of localization to intracellular vesicles that did not label with the ER marker calnexin. In contrast the C214S mutant localized both to ER and intracellular vesicles suggesting that a portion of the mutants passed through the quality control of the ER and accumulated in intracellular vesicles. The P216L mutant was also present both in the ER and in intracellular vesicles.

The biochemical properties of these proteins were also examined on SDS gels under reducing conditions. Figure 6B shows that P216L peripherin-2-GFP migrated more slowly than either the WT or C214S fusion proteins. After PNGase F treatment to remove N-linked oligosaccharides, all proteins migrated at the same rate, slightly ahead of the untreated WT and C214S peripherin-2-GFP. These studies indicate that WT and the C214S mutant are glycosylated and the P216L mutant is hyperglycosylated.

Velocity Sedimentation Analysis of P216L and C214S Peripherin-2

Previously, the oligomeric states of bovine WT, C150S, and L185P peripherin-2 mutants were determined by velocity sedimentation analysis (Loewen and Molday, 2000; Loewen *et al.*, 2001). We have used this technique to examine the effect of the P216L and C214S mutations on the oligomeric structure of peripherin-2 (Figure 7, A and B). Like WT peripherin-2, the P216L mutant sedimented as a mixture of core tetramers (species a), consisting of noncovalently asso-

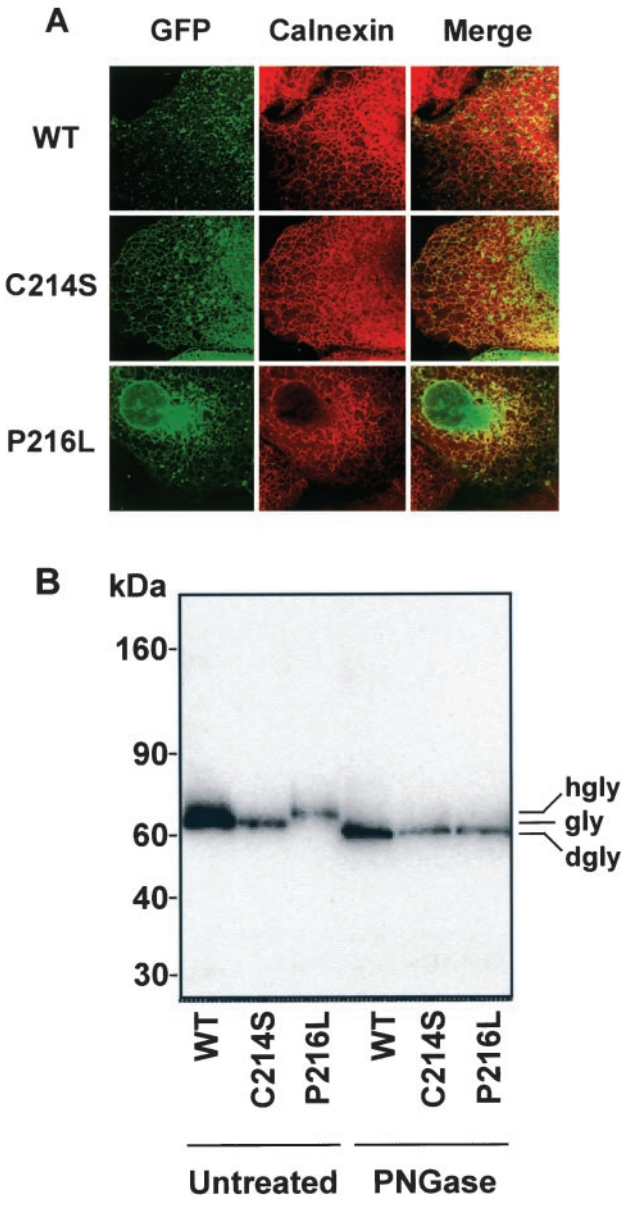

Figure 6. Expression and biochemical properties of *Xenopus* peripherin-2-GFP in cultured COS cells. (A) Confocal micrographs of COS cells expressing WT, C214S, or P216L *Xenopus* peripherin-2-GFP (XPer-GFP) and labeled with an anticalnexin antibody as an ER marker. WT peripherin-2 and a portion of the mutants are present in intracellular vesicles that do not label for calnexin. A significant fraction of the C214S mutant as well as L216P, however, is retained in the ER. (B) Membranes from cells transfected with wild-type (WT), C214S or P216L peripherin-2-GFP were solubilized and incubated in the presence or absence of PNGase. Peripherin-2 was resolved by SDS gel electrophoresis and detected on Western blots labeled with an anti-GFP antibody. A small shift in glycosylated (gly) WT and C214S peripherin-2 and hyperglycosylated (hgly) P216L peripherin-2 to its deglycosylated (dgly) form is observed after treatment with PNGase.

ciated monomeric subunits, and higher order oligomers (species b), comprised of disulfide-linked dimers (Loewen and Molday, 2000). This suggests that the bovine P216L mutation does not adversely affect the assembly of peripherin-2 into core tetramers or higher order disulfide-linked oligomers. The C214S mutant sedimented with a distinctly different profile. Under nonreducing conditions, it sedimented as a mixture of noncovalent dimers (species c), tetramers composed of two disulfide-linked dimers (species d), and aggregated, disulfide-linked species not found for WT or P216L peripherin-2.

DISCUSSION

In this study we have expressed WT and mutant peripherin-2-GFP fusion proteins in rod photoreceptors of *X. laevis* tadpoles and COS-1 cells in order to determine the effect of selected missense mutations in the large EC-2 domain on 1) the targeting of peripherin-2 to ROS disks, 2) outer segment structure, 3) photoreceptor degeneration, and 4) subunit assembly. Our results, together with earlier biochemical characterization of peripherin-2 mutants, indicate that noncovalent core tetramer formation is required for the transport and incorporation of peripherin-2 into nascent disks as summarized in Figure 8. This has important implications in understanding molecular mechanisms underlying peripherin-2–mediated ADRP.

WT Peripherin-2-GFP Exhibits Normal Biochemical Properties and Targeting to Disk Rims and Incisures

To validate the use of peripherin-2 containing a C-terminal GFP tag in transgenic studies, we first examined the biochemical properties and subcellular distribution of WT peripherin-2-GFP in COS-1 cells. Both bovine and *Xenopus* peripherin-2-GFP exhibited properties similar to WT peripherin-2 without GFP when analyzed by covalent cross-linking, immunoprecipitation, migration behavior on reducing and nonreducing SDS gels, and fluorescence microscopy. On this basis, we conclude that GFP fused to the C termini of peripherin-2 does not affect noncovalent tetramer formation or disulfide-linked oligomerization. This is consistent with earlier studies showing that the EC-2 domain, and not the C termini, of peripherin-2, is important in tetramerization and disulfide-linked oligomerization (Goldberg and Molday, 1996a; Goldberg *et al.*, 1998; Loewen and Molday, 2000; Loewen *et al.*, 2001). The finding that bovine and *Xenopus* peripherin-2 associate with one another when coexpressed in COS-1 cells further indicates that the conformation of the EC-2 domain of these orthologues is similar. This is consistent with the high degree of sequence identity between bovine and *Xenopus* peripherin-2 (72% overall identity and 83% identity within the EC-2 domain). Finally, peripherin-2-GFP is found in vesicles within COS-1 cells, indicating that, like peripherin-2, the fusion protein passes through the quality control system of the ER.

Like endogenous peripherin-2, bovine and *Xenopus* peripherin-2-GFP fusion proteins targeted specifically to the rims and incisures of ROS disks at moderate expression levels without affecting ROS structure or inducing photoreceptor degeneration. This indicates that the GFP tag does not affect peripherin-2 trafficking to the disk rims and incisures

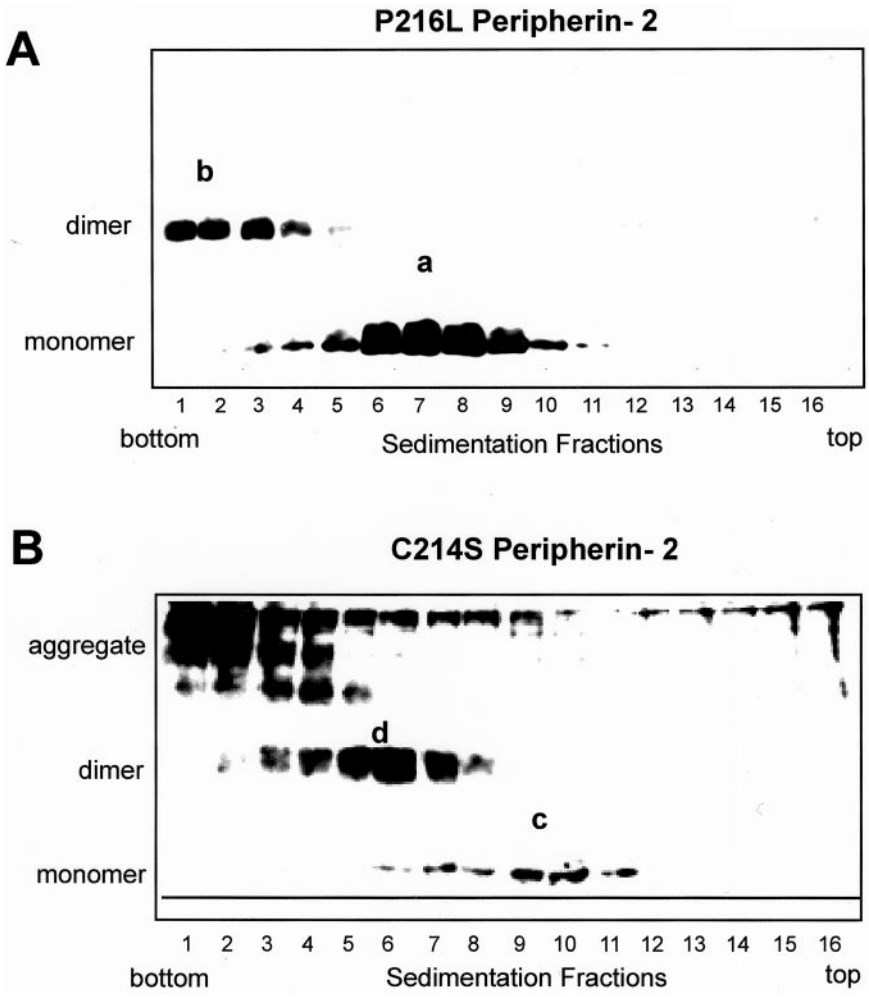

Figure 7. Velocity sedimentation of P216L and C214S peripherin-2 mutants under nonreducing conditions. COS-1 cells expressing bovine P216L (A) and C214S mutant (B) were solubilized in Triton X-100 and subjected to velocity sedimentation. Western blots of the fractions run on nonreducing SDS gels were labeled with the Per2B6 peripherin-2 antibody. The P216L peripherin-2 exhibits a profile consisting of noncovalent tetramers (a) and higher order disulfide-linked oligomers (b) similar to that observed for WT peripherin-2 (Loewen and Molday, 2000). The C214S peripherin-2 produces a mixture of noncovalent dimers (c), tetramers composed of disulfide-linked dimers (d), and aggregated species that sediment near the bottom of the tube.

or ROS organization. At high expression levels, however, a portion of the peripherin-2-GFP is observed in the lamellar region of disks. This abnormal localization is likely due to the inability of the rims and incisures to accommodate excessive amounts of peripherin-2-GFP. A constriction in the diameter of the outer segment and shortening and disorganization of the disks also correlates with high peripherin-2-GFP expression. In contrast, enlarged disks have been observed when peripherin-2 (or rom-1) expression is low or absent (Hawkins *et al.*, 1984; Kedzierski *et al.*, 1997; Clarke *et al.*, 2000). Therefore, peripherin-2 expression levels appear to play a central role in establishing the size of the disks, possibly by controlling disk closure during morphogenesis. In such a case, excess peripherin-2 would increase the rate of closure resulting in smaller disks, whereas low levels would decrease the rate of closure leading to larger disks.

Tetramerization Is Required for Peripherin-2 Targeting to ROS Disks

Our studies indicate that there is a direct correlation between the assembly of peripherin-2 into core noncovalent tetramers and the ability of this complex to target to outer segment disk membranes. WT and P216L peripherin-2, which assemble into core noncovalent tetramers and disulfide-linked oligomers as measured by velocity sedimentation in this and previous studies (Goldberg and Molday, 1996b; Loewen and Molday, 2000), targeted normally to the rims and incisures of ROS disk membranes. The C150S mutant, which forms tetramers, but not disulfide-linked oligomers (Loewen and Molday, 2000), also targeted to disks, indicating that disulfide-linked oligomerization is not required for the incorporation of peripherin-2 into disks.

In contrast tetramerization-defective mutants were not targeted to ROS. The C214S mutant, which forms homodimers but fails to form tetramers even with WT peripherin-2, is retained in the cell body, and inner segment of the rod cells. The L185P mutant, which exists as a mixture of homodimers and heterotetramers with WT peripherin-2 (Loewen *et al.*, 2001), localized to both the rod outer and inner segments. The fraction of L185P peripherin-2 found in ROS disks most likely corresponds to L185P peripherin-2-GFP that associates with endogenous *Xenopus* peripherin-2 to form tetramers, whereas the fraction that is retained in the inner segments and cell body represents L185P peripherin-2 that exists as homodimers.

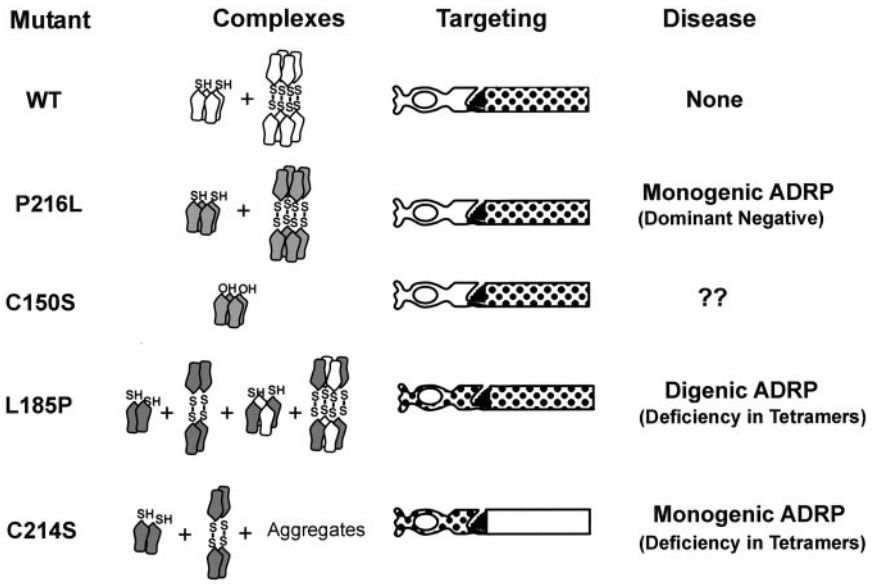

Figure 8. Schematic summarizing the relationship between peripherin-2 subunit assembly, targeting and ADRP. WT (white) and the P216L (shaded) peripherin-2, which form a mixture of core tetramers and disulfide-linked oligomers in association with endogenous *X. laevis* peripherin-2, target normally to ROS disks (patterned region). The P216L mutant causes ADRP through a dominant negative mechanism. The C150S mutant, which forms core tetramers but not disulfide-linked oligomers, also targets to ROS disks. The L185P mutant forms homodimers and disulfide-linked tetramers, which are retained in the inner segment, and noncovalent tetramers and oligomers with WT peripherin-2, which target to ROS. The C214S mutant forms homodimers, disulfide-linked tetramers and aggregates. These complexes are retained in the cell body, inner segments and cilium. The C214S and L185P mutants cause ADRP through a deficiency in functional core tetramers.

On the basis of these results and COS-1 expression studies, we suggest that rod photoreceptors have two quality control mechanisms to assure that only peripherin-2 tetramers traffick to the outer segment and get incorporated into disk membranes. First, photoreceptors, like other cells, have a quality control mechanism to retain grossly misfolded proteins in the ER or inclusion bodies known as aggresomes for eventual degradation (Sung *et al.,* 1991; Illing *et al.,* 2002; Saliba *et al.,* 2002). However, a portion of poorly assembled peripherin-2 mutants (C214S and L185P mutants) exits the ER as shown by their presence in intracellular vesicles in COS-1 cells and at the apical region of the rod inner segment near the base of the cilium, an area in the rod cell that is rich in post-Golgi vesicles, but devoid of ER and Golgi (Papermaster *et al.,* 1985; Deretic and Papermaster, 1991; Moritz *et al.,* 2001a). Another checkpoint in the vicinity of the connecting cilium prevents these tetramerization-defective proteins from becoming incorporated into nascent disk membranes of the ROS. As a result, these proteins remain in the inner segment where they do not affect outer segment morphogenesis or structure.

By analogy with rhodopsin (Marszalek *et al.,* 2000), a model for the transport of peripherin-2 from the inner to the outer segment can be envisioned (Figure 9). WT peripherin-2 together with a fraction of the tetramerization-defective variants are processed through the ER and Golgi and exit in post-Golgi vesicles, distinct from rhodopsin-containing vesicles (Fariss *et al.,* 1997). Tetramerization-competent peripherin-2 is transported through the cilium by a kinesin-dependent mechanism (Marszalek *et al.,* 2000) and incorporated into nascent disks, whereas mutant dimers are retained in the inner segment. The mechanism that prevents incompletely assembled peripherin-2 from targeting to the outer segment is not known, but it may involve the inability of dimeric peripherin-2 to associate with accessory proteins required for trafficking through the cilium. Mechanisms that link subunit assembly to cell membrane targeting have been reported for other multisubunit transmembrane proteins, including K channels and GABA receptors (Zerangue *et al.,* 1999; Manganas and Trimmer, 2000; Margeta-Mitrovic *et al.,* 2000).

ADRP Associated with the C214S and L185P Peripherin-2 Mutations Results from a Deficiency in WT Peripherin-2

The C214S mutation in peripherin-2 is responsible for photoreceptor cell death in individuals with this monogenic form of ADRP (Saga *et al.,* 1993). Studies carried out here, however, indicate that expression of the C214S peripherin-2 on a WT peripherin-2 background does not, itself, affect ROS structure or induce photoreceptor degeneration. This suggests that photoreceptor degeneration in individuals with the C214S mutation results primarily from a deficiency in WT peripherin-2 similar to photoreceptor degeneration displayed in heterozygous *rds* mice (Hawkins *et al.,* 1984; Cheng *et al.,* 1997) and individuals with a peripherin-2 null allele (Jacobson *et al.,* 1996). The possibility that long-term accumulation of misfolded C214S peripherin-2 in rod inner segments and cilium further contributes to photoreceptor degeneration in these individuals, however, cannot be ruled out.

Digenic ADRP linked to the L185P peripherin-2 mutation also appears to occur through a deficiency in WT peripherin-2 because L185P peripherin-2-GFP expression does not affect ROS structure or induce photoreceptor degeneration in our system. In this instance, individuals who inherit the L185P peripherin-2 mutation along with a rom-1 null allele (Kajiwara *et al.,* 1994) will have levels of functional peripherin-2 containing tetramers below the threshold required to sustain disk morphogenesis and photoreceptor viability and as a result will be affected with ADRP. In contrast individuals who inherit only the L185P peripherin-2 mutation will be essentially normal since L185P peripherin-2 can associate with rom-1 and WT peripherin-2 to generate sufficient levels of functional tetramers to support ROS disk morphogenesis (Goldberg and Molday, 1996a; Loewen *et al.,* 2001). In transgenic *X. laevis*, there is sufficient WT peripherin-2 to support

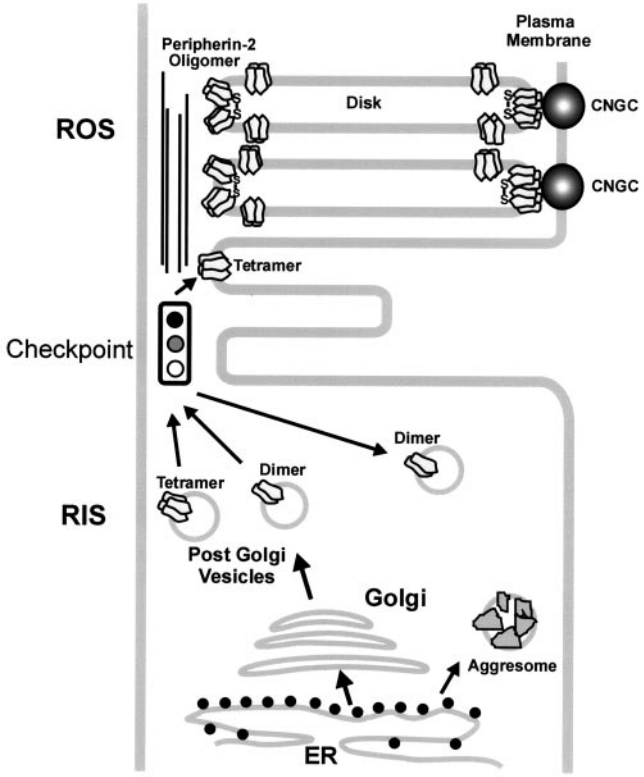

Figure 9. Model depicting a checkpoint that allows only correctly assembled peripherin-2 tetramers to be incorporated into nascent disks. Peripherin-2 tetramers and a significant fraction of dimers are processed through the ER and Golgi and exit as peripherin-2–containing post-Golgi vesicles in the rod inner segment (RIS). These vesicles are translocated to the base of the connecting cilium. A checkpoint prevents peripherin-2 dimers (C214S and L185P homodimers) from being incorporated into the rod outer segment (ROS) disks. Peripherin-2 tetramers and disulfide-linked oligomers, however, are incorporated into nascent disks and localize to the rims and incisures of mature disks. Interaction of peripherin-2 in the disk rim with the cyclic nucleotide-gated channel (CNGC) in the plasma membrane is also shown (Poetsch *et al.,* 2001).

disk morphogenesis and as a result photoreceptor degeneration is not observed in these transgenic animals. Recently, Kedzierski *et al.* (2001) have also suggested that a deficiency in peripherin-2 underlies digenic ADRP on the basis of the phenotypes of mice harboring the L185P and/or rom-1 null mutations, although the molecular basis or targeting aspects were not addressed in this study.

ADRP Associated with the P216L Peripherin-2 Mutation Occurs through a Dominant Negative Mechanism

The P216L peripherin-2-GFP mutant exhibits distinct properties. It targets specifically to the rims and incisures of *Xenopus* ROS disks similar to WT peripherin-2, suggesting that the mutant protein, perhaps in association with endogeneous WT peripherin-2, is properly folded so as to pass through the quality control system of the rod cell. In COS-1 cells, however, only a portion of the *Xenopus* P216L GFP fusion protein exits the ER into intracellular vesicles, indicating that in this cell environment not all the mutant is properly folded. Evidently coassembly of the P216L mutant with endogenous WT peripherin-2 in rod cells and/or the presence of photoreceptor specific chaperone proteins facilitates the proper folding of the mutant and the effective translocation of the peripherin-2 complex from the ER to the ROS disks. However, unlike the C214S and L185P mutants, P216L peripherin-2-GFP has a profound effect on photoreceptors. Peripheral rod cells of 4-week-old *X. laevis* tadpoles expressing the P216L mutant appear normal with proper targeting of the P216L peripherin-2-GFP to the disk rims and incisures. In contrast, central rod cells have short, highly disorganized outer segments displaying whorls of disk membrane with clear evidence of photoreceptor degeneration. Photoreceptors of the central retina of *X. laevis* are older than peripheral photoreceptors (Hollyfield, 1971). The differential appearance and degeneration of central and peripheral photoreceptors expressing this mutant may arise from the age difference of these cells. Similar differential degeneration has been observed in *Xenopus* rods expressing rab8 mutants (Moritz *et al.,* 2001a). Analysis of transgenic animals at later stages is required to define the time course of peripheral and central rod degeneration.

The question arises "What is the molecular basis for the dominant negative effect of the P216L mutant on ROS structure and photoreceptor degeneration?" Sequence analysis suggests the possible involvement of N-linked glycosylation. The proline at position 216, which is part of the sequence ^{215}N-P-S^{217}, prevents glycosylation from occurring at asparagine 215 in WT peripherin-2. Substitution of proline with leucine, however, creates a new N-linked glycosylation site ^{215}N-L-S^{217} in peripherin-2. Indeed, *Xenopus* P216L peripherin-2 migrates more slowly than WT peripherin-2 on SDS gels in the absence of PNGase treatment, but not after deglycosylation, suggesting that this site is glycosylated (Figure 6). During our studies, Wrigley *et al.* (2002) have also demonstrated that in vitro expression of P216L peripherin-2 mutant is hyperglycosylated. It is possible that introduction of a bulky oligosaccharide chain at N^{215} of the P216L mutant may lead to ROS disk instability and progressive photoreceptor degeneration.

In summary, our studies indicate peripherin-2 tetramerization is essential for the normal targeting of peripherin-2 to ROS disk membranes. A checkpoint in the vicinity of the cilium prevents poorly assembled peripherin-2 mutants from being incorporated into nascent disks. Individuals with tetramerization-defective mutations (C214S, C167Y, L185P) succumb to ADRP by a mechanism primarily involving a deficiency of WT peripherin-2, similar to heterozygous rds mice, whereas individuals with tetramerization-competent ADRP mutations (P216L) are affected through a dominant negative effect of the mutant on disk morphogenesis and structure. These mechanisms have implications in the design of gene therapy approaches. Individuals with C214S and L185P tetramerization-defective mutations will likely benefit from genetic approaches that simply increase the expression of WT peripherin-2 before photoreceptor degeneration, whereas individuals with a dominant negative mutation

such as P216L will require disruption of the mutant gene in addition to increased expression of the WT gene.

ACKNOWLEDGMENTS

We thank Dr. Lawrence B. Hurd and Laurie Molday for processing of samples for electron microscopy and Dr. Andrew Goldberg for generating the bovine P216L peripherin-2 mutation. This work was supported by grants from the National Institutes of Health (EY02422 and EY6891); Canadian Institutes of Health Research (MT 5822), and the Foundation Fighting Blindness. C.J.R.L. was a recipient of a predoctoral fellowship from the Foundation Fighting Blindness Canada.

REFERENCES

Arikawa, K., Molday, L.L., Molday, R.S., and Williams, D.S. (1992). Localization of peripherin/rds in the disk membranes of cone and rod photoreceptors: relationship to disk membrane morphogenesis and retinal degeneration. J. Cell Biol. *116,* 659–667.

Batni, S., Mani, S.S., Schlueter, C., Ji, M., and Knox, B.E. (2000). Xenopus rod photoreceptor: model for expression of retinal genes. Methods Enzymol. *316,* 50–64.

Bok, D. (1985). Retinal photoreceptor-pigment epithelium interactions. Friedenwald lecture. Invest Ophthalmol. Vis. Sci. *26,* 1659–1694.

Cheng, T., Peachey, N.S., Li, S., Goto, Y., Cao, Y., and Naash, M.I. (1997). The effect of peripherin/rds haploinsufficiency on rod and cone photoreceptors. J. Neurosci. *17,* 8118–8128.

Clarke, G. *et al.* (2000). Rom-1 is required for rod photoreceptor viability and the regulation of disk morphogenesis. Nat. Genet. *25,* 67–73.

Connell, G., Bascom, R., Molday, L., Reid, D., McInnes, R.R., and Molday, R.S. (1991). Photoreceptor peripherin is the normal product of the gene responsible for retinal degeneration in the rds mouse. Proc. Natl. Acad. Sci. USA *88,* 723–726.

Connell, G.J., and Molday, R.S. (1990). Molecular cloning, primary structure, and orientation of the vertebrate photoreceptor cell protein peripherin in the rod outer segment disk membrane. Biochemistry *29,* 4691–4698.

Deretic, D., and Papermaster, D.S. (1991). Polarized sorting of rhodopsin on post-Golgi membranes in frog retinal photoreceptor cells. J. Cell Biol. *113,* 1281–1293.

Fariss, R.N., Molday, R.S., Fisher, S.K., and Matsumoto, B. (1997). Evidence from normal and degenerating photoreceptors that two outer segment integral membrane proteins have separate transport pathways. J. Comp. Neurol. *387,* 148–156.

Farrar, G.J., Kenna, P., Jordan, S.A., Kumar-Singh, R., Humphries, M.M., Sharp, E.M., Sheils, D.M., and Humphries, P. (1991). A three-base-pair deletion in the peripherin-RDS gene in one form of retinitis pigmentosa. Nature *354,* 478–480.

Goldberg, A.F., Loewen, C.J., and Molday, R.S. (1998). Cysteine residues of photoreceptor peripherin/rds: role in subunit assembly and autosomal dominant retinitis pigmentosa. Biochemistry *37,* 680–685.

Goldberg, A.F., and Molday, R.S. (1996a). Defective subunit assembly underlies a digenic form of retinitis pigmentosa linked to mutations in peripherin/rds and rom-1. Proc. Natl. Acad. Sci. USA *93,* 13726–13730.

Goldberg, A.F., and Molday, R.S. (1996b). Subunit composition of the peripherin/rds-rom-1 disk rim complex from rod photoreceptors: hydrodynamic evidence for a tetrameric quaternary structure. Biochemistry *35,* 6144–6149.

Goldberg, A.F., Moritz, O.L., and Molday, R.S. (1995). Heterologous expression of photoreceptor peripherin/rds and Rom-1 in COS-1 cells: assembly, interactions, and localization of multisubunit complexes. Biochemistry *34,* 14213–14219.

Hawkins, R.K., Jansen, H.G., and Sanyal, S. (1984). Development and degeneration of retina in rds mutant mice: photoreceptor abnormalities in the heterozygotes. Exp. Eye Res. *41,* 701–720.

Hemler, M.E. (2001). Specific tetraspanin functions. J. Cell Biol. *155,* 1103–1107.

Hollyfield, J.G. (1971). Differential growth of the neural retina in *Xenopus laevis* larvae. Dev. Biol. *24,* 264–286.

Illing, M.E., Rajan, R.S., Bence, N.F., and Kopito, R.R. (2002). A rhodopsin mutant linked to autosomal dominant retinitis pigmentosa is prone to aggregate and interacts with the ubiquitin proteasome system. J. Biol. Chem. *277,* 34150–34160.

Jacobson, S.G., Cideciyan, A.V., Kemp, C.M., Sheffield, V.C., and Stone, E.M. (1996). Photoreceptor function in heterozygotes with insertion or deletion mutations in the RDS gene. Invest. Ophthalmol. Vis. Sci. *37,* 1662–1674.

Kajiwara, K., Berson, E.L., and Dryja, T.P. (1994). Digenic retinitis pigmentosa due to mutations at the unlinked peripherin/RDS and ROM1 loci. Science *264,* 1604–1608.

Kajiwara, K., Hahn, L.B., Mukai, S., Travis, G.H., Berson, E.L., and Dryja, T.P. (1991). Mutations in the human retinal degeneration slow gene in autosomal dominant retinitis pigmentosa. Nature *354,* 480–483.

Karpen, G.H. (1994). Position-effect variegation and the new biology of heterochromatin. Curr. Opin. Genet. Dev. *4,* 281–291.

Kedzierski, W., Lloyd, M., Birch, D.G., Bok, D., and Travis, G.H. (1997). Generation and analysis of transgenic mice expressing P216L-substituted rds/peripherin in rod photoreceptors. Invest. Ophthalmol. Vis. Sci. *38,* 498–509.

Kedzierski, W., Moghrabi, W.N., Allen, A.C., Jablonski-Stiemke, M.M., Azarian, S.M., Bok, D., and Travis, G.H. (1996). Three homologs of rds/peripherin in *Xenopus laevis* photoreceptors that exhibit covalent and non-covalent interactions. J. Cell Sci. *109,* 2551–2560.

Kedzierski, W., Nusinowitz, S., Birch, D., Clarke, G., McInnes, R.R., Bok, D., and Travis, G.H. (2001). Deficiency of rds/peripherin causes photoreceptor death in mouse models of digenic and dominant retinitis pigmentosa. Proc. Natl. Acad. Sci. USA *98,* 7718–7723.

Kroll, K.L., and Amaya, E. (1996). Transgenic *Xenopus* embryos from sperm nuclear transplantations reveal FGF signaling requirements during gastrulation. Development *122,* 3173–3183.

Loewen, C.J., and Molday, R.S. (2000). Disulfide-mediated oligomerization of Peripherin/Rds and Rom-1 in photoreceptor disk membranes. Implications for photoreceptor outer segment morphogenesis and degeneration. J. Biol. Chem. *275,* 5370–5378.

Loewen, C.J., Moritz, O.L., and Molday, R.S. (2001). Molecular characterization of peripherin-2 and rom-1 mutants responsible for digenic retinitis pigmentosa. J. Biol. Chem. *276,* 22388–22396.

MacKenzie, D., and Molday, R.S. (1982). Organization of rhodopsin and a high molecular weight glycoprotein in rod photoreceptor disc membranes using monoclonal antibodies. J. Biol. Chem. *257,* 7100–7105.

Manganas, L.N., and Trimmer, J.S. (2000). Subunit composition determines Kv1 potassium channel surface expression. J. Biol. Chem. *275,* 29685–29693.

Margeta-Mitrovic, M., Jan, Y.N., and Jan, L.Y. (2000). A trafficking checkpoint controls GABA(B) receptor heterodimerization. Neuron *27,* 97–106.

Marszalek, J.R., Liu, X., Roberts, E.A., Chui, D., Marth, J.D., Williams, D.S., and Goldstein, L.S. (2000). Genetic evidence for selective transport of opsin and arrestin by kinesin-II in mammalian photoreceptors. Cell *102,* 175–187.

Molday, R.S., Hicks, D., and Molday, L. (1987). Peripherin. A rim-specific membrane protein of rod outer segment discs. Invest. Ophthalmol. Vis. Sci. *28,* 50–61.

Moritz, O.L., Tam, B.M., Hurd, L.L., Peranen, J., Deretic, D., and Papermaster, D.S. (2001a). Mutant rab8 impairs docking and fusion of rhodopsin-bearing post-Golgi membranes and causes cell death of transgenic Xenopus rods. Mol. Biol. Cell *12,* 2341–2351.

Moritz, O.L., Tam, B.M., Knox, B.E., and Papermaster, D.S. (1999). Fluorescent photoreceptors of transgenic Xenopus laevis imaged in vivo by two microscopy techniques. Invest. Ophthalmol. Vis. Sci. *40,* 3276–3280.

Moritz, O.L., Tam, B.M., Papermaster, D.S., and Nakayama, T. (2001b). A functional rhodopsin-green fluorescent protein fusion protein localizes correctly in transgenic *Xenopus laevis* retinal rods and is expressed in a time-dependent pattern. J. Biol. Chem. *276,* 28242–28251.

Papermaster, D.S., Schneider, B.G., and Besharse, J.C. (1985). Vesicular transport of newly synthesized opsin from the Golgi apparatus toward the rod outer segment. Ultrastructural immunocytochemical and autoradiographic evidence in *Xenopus* retinas. Invest. Ophthalmol. Vis. Sci. *26,* 1386–1404.

Poetsch, A., Molday, L.L., and Molday, R.S. (2001). The cGMP-gated channel and related glutamic acid-rich proteins interact with peripherin-2 at the rim region of rod photoreceptor disc membranes. J. Biol. Chem. *276,* 48009–48016.

Saga, M., Mashima, Y., Akeo, K., Oguchi, Y., Kudoh, J., and Shimizu, N. (1993). A novel Cys-214-Ser mutation in the peripherin/RDS gene in a Japanese family with autosomal dominant retinitis pigmentosa. Hum. Genet. *92,* 519–521.

Saliba, R.S., Munro, P.M., Luthert, P.J., and Cheetham, M.E. (2002). The cellular fate of mutant rhodopsin: quality control, degradation and aggresome formation. J. Cell Sci. *115,* 2907–2918.

Sanyal, S., and Jansen., H.G. (1981). Absence of receptor outer segments in the retina of rds mutant mice. Neurosci. Lett. *21,* 23–26.

Seigneuret, M., Delaguillaumie, A., Lagaudriere-Gesbert, C., and Conjeaud, H. (2001). Structure of the tetraspanin main extracellular domain. A partially conserved fold with a structurally variable domain insertion. J. Biol. Chem. *276,* 40055–40064.

Sung, C.H., Schneider, B.G., Agarwal, N., Papermaster, D.S., and Nathans, J. (1991). Functional heterogeneity of mutant rhodopsins responsible for autosomal dominant retinitis pigmentosa. Proc. Natl. Acad. Sci. USA *88,* 8840–8844.

Tam, B.M., Moritz, O.L., Hurd, L.B., and Papermaster, D.S. (2000). Identification of an outer segment targeting signal in the COOH terminus of rhodopsin using transgenic Xenopus laevis. J. Cell Biol. *151,* 1369–1380.

Travis, G.H., Brennan, M.B., Danielson, P.E., Kozak, C.A., and Sutcliffe, J.G. (1989). Identification of a photoreceptor-specific mRNA encoded by the gene responsible for retinal degeneration slow (rds). Nature *338,* 70–73.

Travis, G.H., Groshan, K.R., Lloyd, M., and Bok, D. (1992). Complete rescue of photoreceptor dysplasia and degeneration in transgenic retinal degeneration slow (rds) mice. Neuron *9,* 113–119.

Travis, G.H., Sutcliffe, J.G., and Bok, D. (1991). The retinal degeneration slow (rds) gene product is a photoreceptor disc membrane-associated glycoprotein. Neuron *6,* 61–70.

Weleber, R.G., Carr, R.E., Murphey, W.H., Sheffield, V.C., and Stone, E.M. (1993). Phenotypic variation including retinitis pigmentosa, pattern dystrophy, and fundus flavimaculatus in a single family with a deletion of codon 153 or 154 of the peripherin/RDS gene. Arch. Ophthalmol. *111,* 1531–1542.

Wrigley, J.D., Ahmed, T., Nevett, C.L., and Findlay, J.B. (2000). Peripherin/rds influences membrane vesicle morphology. Implications for retinopathies. J. Biol. Chem. *275,* 13191–13194.

Wrigley, J.D., Nevett, C.L., and Findlay, J.B. (2002). Topological analysis of peripherin/rds and abnormal glycosylation of the pathogenic Pro216→Leu mutation. Biochem. J. *368,* 649–655.

Zerangue, N., Schwappach, B., Jan, Y.N., and Jan, L.Y. (1999). A new ER trafficking signal regulates the subunit stoichiometry of plasma membrane K(ATP) channels. Neuron *22,* 537–548.